Research Square

Preprints are preliminary reports that have not undergone peer review.
They should not be considered conclusive, used to inform clinical practice,
or referenced by the media as validated information.

Gestational Diabetes Mellitus Placentas Exhibit Mitonuclear Transcriptional Imbalance Co-occurring with m6A Regulatory Gene Dysregulation: Insights from Bulk RNA Sequencing

Xinyu Zhang
Shanghai Jiao Tong University
Wenxi Tang
University of California San Diego
Linlin Guo
Shanghai Jiao Tong University
Han Bao
Shanghai Jiao Tong University
Xiafang Chen
chxf_1984@hotmail.com

National Children's Medical Center, Shanghai Children's Medical Center, Shanghai Jiao Tong University

Research Article

Keywords: gestational diabetes mellitus, placenta, mitonuclear imbalance, oxidative phosphorylation, N6-methyladenosine, transcriptomics

Posted Date: July 22nd, 2026

DOI: https://doi.org/10.21203/rs.3.rs-10060346/v1

License: This work is licensed under a Creative Commons Attribution 4.0 International License.
Read Full License

Additional Declarations: No competing interests reported.

Gestational Diabetes Mellitus Placentas Exhibit Mitonuclear Transcriptional Imbalance Co-occurring with m6A Regulatory Gene Dysregulation: Insights from Bulk RNA Sequencing

Xinyu Zhang[1], Wenxi Tang[2], Linlin Guo[1], Han Bao[1], Xiafang Chen[3*]

[1] Department of Obstetrics and Gynecology, Renji Hospital, School of Medicine, Shanghai Jiao Tong University, Shanghai 200127, China

[2] School of Medicine, University of California San Diego, La Jolla, CA, United States

[3] Department of Neonatology, National Children's Medical Center, Shanghai Children's Medical Center, Affiliated to School of Medicine Shanghai Jiao Tong University, Shanghai, China

*Correspondence: Xiafang Chen, chxf_1984@hotmail.com

Abstract

Background

Gestational diabetes mellitus (GDM) affects approximately 14% of pregnancies globally and is associated with placental dysfunction and adverse perinatal outcomes. While mitochondrial dysfunction in GDM placentas is well-documented, the coordinated relationship between mitochondrial DNA (mtDNA)-encoded and nuclear genome-encoded oxidative phosphorylation (OXPHOS) gene expression — termed mitonuclear transcriptional imbalance, has not previously been described in this context.

Methods

We performed transcriptomic analysis of bulk RNA-seq data from 14 GDM (GDMA1, n = 5; GDMA2, n = 9) and 11 normoglycemic control placental samples from the publicly available dataset GSE249311. Differential expression analysis was performed using DESeq2. Gene Set Enrichment Analysis (GSEA) was performed using the Hallmark gene set collection. A rank-based Mitonuclear Index was computed using ssGSEA with the predefined Hallmark OXIDATIVE_PHOSPHORYLATION gene set (MSigDB, n = 200 genes) to avoid circularity with differential expression results. Robustness was assessed by leave-one-out analysis and comparison across three scoring algorithms (ssGSEA, GSVA, Z-score module score). Directional consistency was assessed in an independent microarray cohort (GSE70493, n = 63).

Results

All 13 mtDNA-encoded respiratory chain genes were significantly downregulated in GDM placentas ($\log_2$FC ≈ −1.4, adjusted $P < 10^{-9}$), while nuclear-encoded OXPHOS genes were the most significantly upregulated pathway by GSEA (NES = 2.15, adjusted $P = 1.19 \times 10^{-8}$). The Mitonuclear Index was significantly elevated in GDM versus controls (Wilcoxon $P = 8.75 \times 10^{-5}$, rank-biserial r = 0.72) and was consistently observed across GDMA1, GDMA2, and T2DM in pregnancy subtypes. Leave-one-out analysis confirmed robustness across all 25 samples (all

iterations $P < 0.001$). The signal was directionally concordant across alternative scoring approaches, though statistical support varied by method (ssGSEA $P < 0.001$; Z-score $P = 0.044$; GSVA $P = 0.066$). Six m6A regulatory genes were significantly dysregulated, including upregulation of METTL14, WTAP, and RBM15, co-occurring with the mitonuclear transcriptional state.

Conclusions

These findings suggest mitonuclear transcriptional imbalance as a candidate placental transcriptional phenotype associated with maternal hyperglycemia. Future mechanistic studies are warranted to determine whether impaired mtDNA transcription, retrograde mitochondrial signaling, and m6A epitranscriptomic remodeling jointly contribute to placental adaptation in GDM.

Keywords: gestational diabetes mellitus; placenta; mitonuclear imbalance; oxidative phosphorylation; N6-methyladenosine; transcriptomics

1. Introduction

Gestational diabetes mellitus (GDM) is defined as glucose intolerance first diagnosed during pregnancy at concentrations below the threshold for overt diabetes. It is among the most common pregnancy complications, affecting approximately 14% of pregnancies globally, with prevalence continuing to rise in parallel with obesity and type 2 diabetes[1]. GDM is associated with a range of adverse maternal and fetal outcomes, including preeclampsia, cesarean delivery, macrosomia, neonatal hypoglycemia, and increased long-term risk of type 2 diabetes in both mother and offspring[2]. Beyond these immediate clinical consequences, emerging evidence suggests that GDM induces lasting molecular alterations in the placenta that may mediate fetal programming and intergenerational transmission of metabolic risk[3].

The placenta serves as the primary interface for nutrient and oxygen transfer between mother and fetus, and its proper function is critically dependent on mitochondrial energy metabolism. Placental mitochondrial dysfunction has been well-documented in GDM, with evidence of reduced oxidative phosphorylation capacity, impaired electron transport chain complex expression, increased reactive oxygen species (ROS) production, and oxidative DNA damage[4]. However, the coordinated relationship between mitochondrial DNA (mtDNA)-encoded and nuclear genome-encoded gene expression in GDM placentas has not been systematically examined. The OXPHOS system is unique in that its constituent protein complexes are encoded by both genomes, requiring

precise transcriptional coordination across compartments. Dysregulation of this balance termed mitonuclear transcriptional imbalance has been implicated in aging, obesity, and type 2 diabetes, but has not previously been described in the context of GDM placentas[5,6].

N6-methyladenosine (m6A) modification is the most abundant internal modification on mammalian mRNA and plays critical roles in regulating RNA stability, translation, and splicing. m6A modification is dynamically regulated by writer complexes (including METTL3, METTL14, and WTAP), eraser enzymes (FTO and ALKBH5), and reader proteins (YTHDF and IGF2BP families). Emerging evidence has implicated m6A dysregulation in gestational complications: METTL14 upregulation contributes to trophoblast dysfunction in preeclampsia[7], METTL3 is essential for trophoblast stem cell self-renewal during placentation[8], and m6A modification has been shown to regulate mitochondrial homeostasis through modulation of OXPHOS complex subunit translation efficiency[9]. Whether m6A epitranscriptomic remodeling co-occurs with mitochondrial transcriptional dysregulation in GDM placentas has not been investigated.

Despite these advances, a comprehensive characterization of the transcriptional landscape linking mitochondrial gene expression, nuclear OXPHOS coordination, and m6A regulatory gene expression in GDM placentas is lacking. The availability of publicly accessible high-quality RNA-seq datasets from well-characterized GDM cohorts provides an opportunity to address this gap through transcriptome-wide analysis. In particular, the recent GSE249311 dataset[10] offers bulk RNA-seq data from carefully subtyped GDM placentas (GDMA1 and GDMA2), enabling both subtype-specific and broader analyses of the hyperglycemic placental transcriptome.

In this study, we performed systematic transcriptomic analysis of GDM placentas using GSE249311, with the specific aims of: (1) characterizing the genome-wide differential expression landscape in GDM versus normoglycemic placentas; (2) investigating whether mitonuclear transcriptional imbalance represents a consistent placental phenotype across hyperglycemic subtypes; (3) quantifying this imbalance using a platform-agnostic rank-based Mitonuclear Index and assessing its internal consistency across subgroups and directional consistency in an independent cohort; and (4) characterizing the m6A regulatory gene expression landscape in GDM placentas and its relationship to the mitonuclear transcriptional state.

2. Materials and Methods

2.1 Data Source and Sample Selection

The RNA sequencing dataset GSE249311 was obtained from the Gene Expression Omnibus (GEO) public database (https://www.ncbi.nlm.nih.gov/geo/). This dataset contains bulk RNA-seq data from human term placental tissue, originally generated by Barrozo et al. (2024) and deposited under accession GSE249311. The raw count matrix (GSE249311_count_matrix.tsv.gz) was downloaded directly from the GEO supplementary files. The original dataset includes samples classified as gestational diabetes subtype A1 (GDMA1, diet-controlled; n = 5), gestational diabetes subtype A2 (GDMA2, medication-requiring; n = 9), type 2 diabetes mellitus in pregnancy (T2DM; n = 5), unknown subtype (UNK; n = 24), and normoglycemic controls (n = 11). For the primary analysis, only samples with confirmed gestational diabetes mellitus (GDMA1 and GDMA2, collectively referred to as GDM; n = 14) and normoglycemic controls (n = 11) were included, yielding 25 samples. T2DM and UNK samples were excluded from the primary differential expression analysis to ensure diagnostic homogeneity, but T2DM samples were retained for internal subgroup assessment (Section 2.7).

2.2 Differential Expression Analysis

Differential expression analysis was performed using the DESeq2 package (v1.38.0) in R (v4.5.1)[11]. Raw read counts were used as input. Genes with fewer than 10 counts in fewer than 3 samples were removed prior to analysis. Size factor estimation, dispersion estimation, and negative binomial modeling were performed according to the standard DESeq2 workflow. Genes with a $\log^2$ fold change ($|\log^2 FC| > 1$) and an adjusted P value (Benjamini–Hochberg correction) less than 0.05 were considered differentially expressed genes (DEGs). Log^2-transformed normalized counts ($\log^2[\text{count} + 1]$) were used for downstream score calculations.

2.3 Gene Set Enrichment Analysis (GSEA)

Gene Set Enrichment Analysis (GSEA) was performed using the clusterProfiler package (v4.6.0) in R[12]. All expressed genes were ranked by their DESeq2 Wald test statistic in descending order. The Hallmark gene set collection from the Molecular Signatures Database (MSigDB, v2023.2)[13] was accessed via the msigdbr package (v7.5.1). GSEA was run with 1,000 permutations, a minimum gene set size of 15, and a maximum gene set size of 500. Gene sets with an adjusted P value less than 0.05 were considered significantly enriched.

2.4 Mitonuclear Imbalance Quantification

To quantify mitonuclear transcriptional imbalance in a platform-agnostic manner, both the mtDNA module score and the Nuclear OXPHOS score were computed using single-sample gene set enrichment analysis (ssGSEA), implemented via the GSVA package (v1.46.0) [14]. This rank-based approach was chosen over raw expression averaging to ensure comparability across different transcriptomic platforms.

The mtDNA module comprised 13 mitochondrial DNA-encoded genes: *MT-ND1, MT-ND2, MT-ND3, MT-ND4, MT-ND4L, MT-ND5, MT-ND6, MT-CO1, MT-CO2, MT-CO3, MT-CYB, MT-ATP6*, and *MT-ATP8*. The Nuclear OXPHOS module comprised all 200 genes in the Hallmark OXIDATIVE_PHOSPHORYLATION gene set from MSigDB (v2023.2), which are exclusively nuclear genome-encoded. This predefined, data-independent gene set was chosen to avoid circularity between module definition and differential expression results. The Mitonuclear Index was defined as the difference between the Nuclear OXPHOS ssGSEA score and the mtDNA ssGSEA score for each sample:

Mitonuclear Index = Nuclear OXPHOS score (ssGSEA) − mtDNA score (ssGSEA)

A higher Mitonuclear Index indicates greater relative upregulation of the nuclear OXPHOS program relative to mtDNA-encoded gene expression. Group differences in the Mitonuclear Index were assessed using two-tailed Wilcoxon rank-sum tests. Effect size was reported as rank-biserial correlation.

2.5 Analysis of m6A Regulatory Gene Expression

A panel of 16 well-characterized m6A regulatory genes was selected, comprising writers (*METTL3, METTL14, WTAP, RBM15, ZC3H13, METTL16*), erasers (*FTO, ALKBH5*), and readers (*YTHDF1, YTHDF2, YTHDF3, YTHDC1, YTHDC2, IGF2BP1, IGF2BP2, IGF2BP3*). Differential expression of these genes was extracted from the DESeq2 results and visualized using bubble plots and heatmaps with Z-score scaling applied per gene.

2.6 Correlation Analysis

To explore the relationship between m6A regulatory gene expression and the mitonuclear transcriptional state, Pearson correlation analysis was performed between *METTL14* $\log^2$-

normalized expression and the Mitonuclear Index across all 25 primary analysis samples using the cor.test function in R. The Nuclear OXPHOS module used to compute the Mitonuclear Index was the predefined Hallmark OXIDATIVE_PHOSPHORYLATION gene set from MSigDB (n = 200 genes), selected independently of the differential expression results and independently of any correlation analysis with *METTL14*. To assess whether the observed correlation was specific to the Nuclear OXPHOS module or reflected a general co-expression pattern among upregulated genes in GDM, a permutation test was performed: 1,000 random gene sets of the same size (n = 200) were drawn from all expressed genes in the dataset (rather than only upregulated DEGs, since the Hallmark OXPHOS set is not restricted to upregulated genes), and the mean expression score of each random set was correlated with *METTL14* expression. The empirical distribution of correlation coefficients was compared with the observed value. Additionally, Pearson correlation was computed between *METTL14* expression and the mtDNA module score to assess directionality. A two-tailed P value less than 0.05 was considered statistically significant.

2.7 Internal Subgroup Assessment across Diabetes Subtypes

To assess the robustness of mitonuclear transcriptional imbalance across different forms of pregnancy-associated hyperglycemia, the Mitonuclear Index was computed for all 30 subtyped samples within GSE249311 (Control n = 11, GDMA1 n = 5, GDMA2 n = 9, T2DM n = 5) using the same ssGSEA methodology described in Section 2.4. Pairwise comparisons between each diabetes subtype and the control group were performed using two-tailed Wilcoxon rank-sum tests.

2.8 Independent Cohort Assessment

To assess the directional consistency of the nuclear OXPHOS upregulation component in an independent cohort (partial external assessment), we analyzed the publicly available placental microarray dataset GSE70493[15] (GDM n = 32, Control n = 31; Affymetrix Human Transcriptome Array 2.0, GPL17586). The Nuclear OXPHOS ssGSEA score was computed using the same Hallmark OXIDATIVE_PHOSPHORYLATION gene set (MSigDB), of which 183 out of 200 genes were present on the Affymetrix HTA 2.0 platform (17 genes were absent from the microarray annotation and excluded). As the Affymetrix HTA 2.0 platform does not include probes for mtDNA-encoded genes, the complete Mitonuclear Index could not be computed in this dataset. Differences in the Nuclear OXPHOS score between GDM and control groups were assessed using a two-tailed Wilcoxon rank-sum test.

2.9 Robustness Analysis

To assess the robustness of the primary findings, three complementary analyses were performed. First, a leave-one-out (LOO) analysis was performed: in each of 25 iterations, one sample was withheld, the Mitonuclear Index was computed for the remaining 24 samples, and group differences were assessed using a two-tailed Wilcoxon rank-sum test. Second, the Mitonuclear Index was recomputed using two alternative scoring algorithms: (i) GSVA, implemented via the gsvaParam function in the GSVA package (v1.46.0), and (ii) a Z-score-based module score, computed as the mean per-sample Z-score of Nuclear OXPHOS module genes minus the mean per-sample Z-score of mtDNA module genes. Both alternative methods used the same predefined Hallmark OXPHOS gene set (MSigDB, n = 200) and mtDNA gene set (n = 13). Pairwise Pearson correlations between the three scoring methods were computed. Third, the mean difference in Nuclear OXPHOS scores between GDM and control groups in GSE70493 was computed, and a 95% bootstrap confidence interval (1,000 resamples, percentile method) was calculated using the boot package (v1.3.28) in R. Effect size was reported as rank-biserial correlation.

2.10 Visualization and Statistical Analysis

All visualizations were generated in R (v4.5.1) using ggplot2, ggrepel, pheatmap, and ggpubr packages. The mitonuclear imbalance heatmap was generated using Z-score-scaled $\log^2$-normalized counts with samples ordered by group. Statistical significance in boxplots was assessed by two-tailed Wilcoxon rank-sum tests. Effect size was reported as rank-biserial correlation.

AI-assisted tools

The authors used Claude (Anthropic; claude.ai, version Claude Sonnet 4.5) to assist with manuscript drafting and language editing during the preparation of this work. All content, analyses, and conclusions were reviewed, verified, and approved by the authors. The AI tool was not used for data analysis, statistical computation, or the generation of scientific conclusions.

3. Results

3.1 Transcriptomic Landscape of GDM Placentas

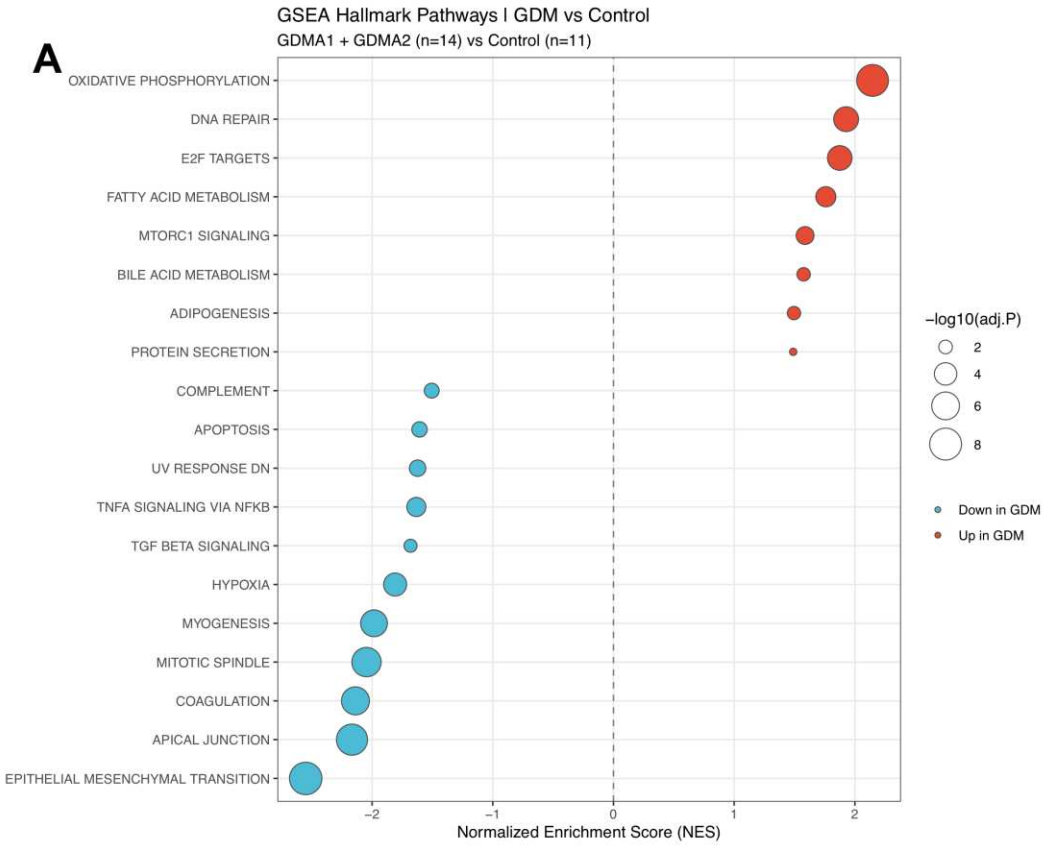
To characterize transcriptomic alterations in GDM placentas, we analyzed bulk RNA-seq data from 14 GDM (GDMA1, n = 5; GDMA2, n = 9) and 11 normoglycemic control placental samples from GSE249311. T2DM and unknown-subtype samples were excluded to ensure diagnostic homogeneity. After filtering low-expression genes, differential expression analysis identified 911 significantly dysregulated genes ($|\log^2 FC| > 1$, adjusted $P < 0.05$): 151 upregulated and 760 downregulated in GDM compared with controls (Figure 1). Among the most significantly downregulated genes were *FN1* ($\log^2 FC = -1.35$, adjusted $P = 2.56 \times 10^{-11}$) and *NEAT1* ($\log^2 FC$

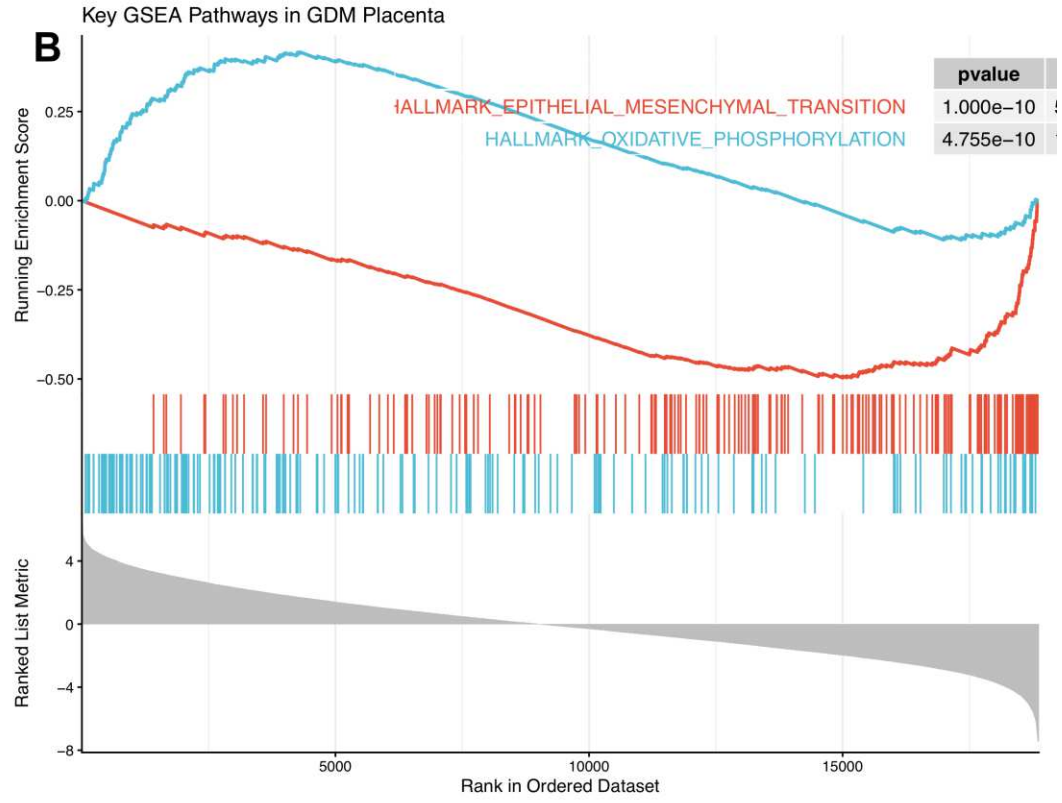
= −1.19, adjusted P = 3.58 × 10^{-9}). Strikingly, all 13 mitochondrial DNA (mtDNA)-encoded respiratory chain genes present in the dataset were significantly downregulated in GDM placentas, including *MT-ND1* through *MT-ND6*, *MT-CO1* through *MT-CO3*, *MT-CYB*, *MT-ATP6*, and *MT-ATP8* (log^2FC ≈ −1.4, adjusted P < 1 × 10^{-9} for all). Conversely, multiple nuclear-encoded mitochondrial proteins were among the top upregulated genes, including ribosomal subunits and electron transport chain assembly factors. This divergent pattern prompted investigation of a potential mitonuclear transcriptional imbalance in GDM placentas.



3.2 GSEA Identifies Nuclear-Encoded Oxidative Phosphorylation as the Most Enriched Pathway

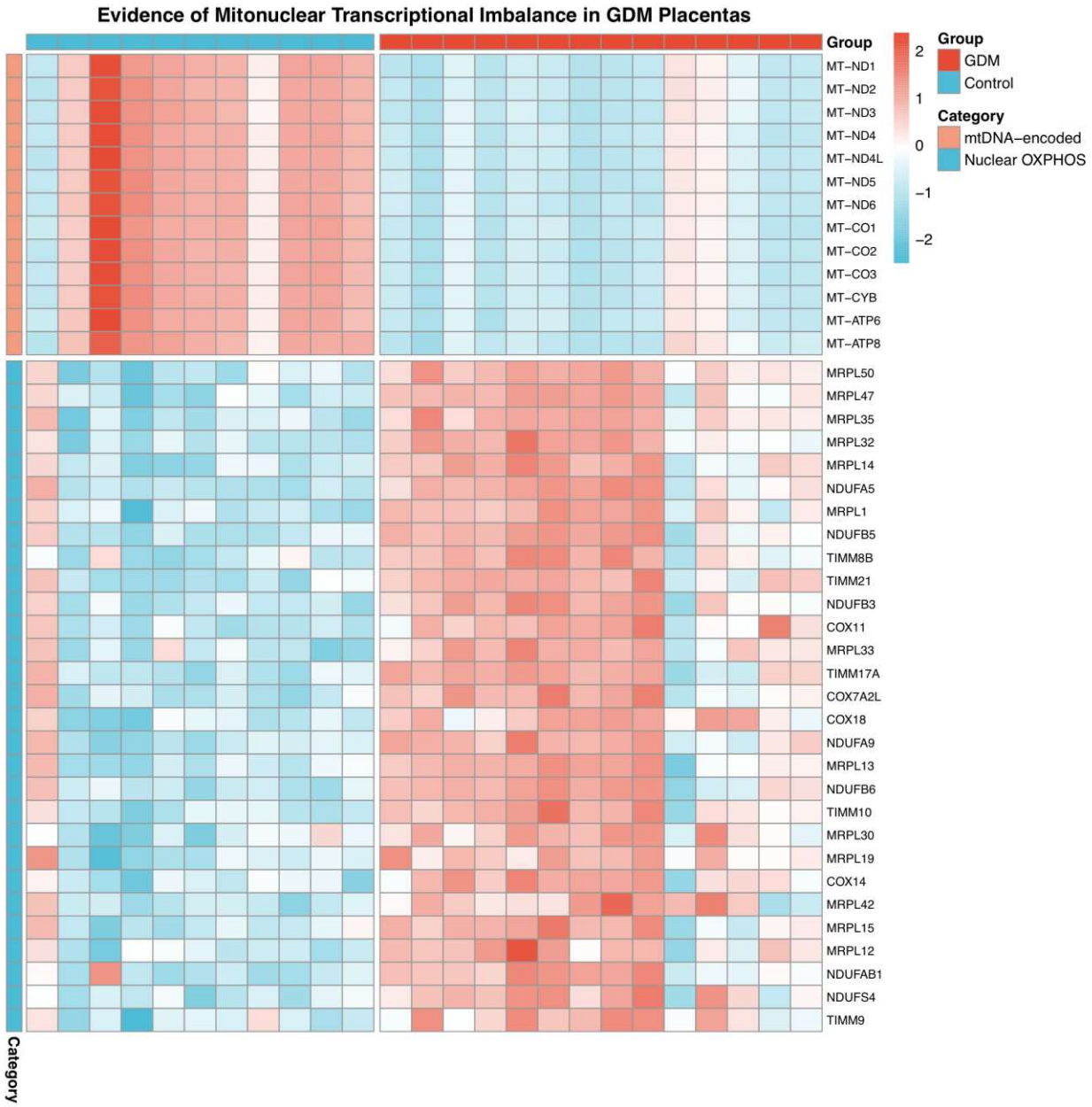
GSEA using the Hallmark gene set collection identified 19 significantly enriched pathways (adjusted $P < 0.05$) (Figure 2A). The most significantly upregulated pathway was HALLMARK_OXIDATIVE_PHOSPHORYLATION (NES = 2.15, adjusted $P = 1.19 \times 10^{-8}$), with leading-edge genes comprising exclusively nuclear genome-encoded mitochondrial proteins, including *MRPL35, TIMM9, NDUFA5, NDUFB5*, and *SDHC* (Figure 2B). None of the 13 mtDNA-encoded respiratory chain genes are represented in the Hallmark OXPHOS gene set, establishing that the GSEA signal reflects upregulation of the nuclear OXPHOS program specifically. Additional significantly upregulated pathways included HALLMARK_FATTY_ACID_METABOLISM (NES = 1.76), HALLMARK_MTORC1_SIGNALING (NES = 1.75), HALLMARK_E2F_TARGETS (NES = 1.87), and HALLMARK_DNA_REPAIR (NES = 1.93). The most significantly downregulated pathway was HALLMARK_EPITHELIAL_MESENCHYMAL_TRANSITION (NES = −2.55, adjusted $P = 5.00 \times 10^{-9}$), alongside HALLMARK_APICAL_JUNCTION (NES = −2.17) and HALLMARK_HYPOXIA (NES = −1.81). Taken together with the DEG results, these findings indicated a co-occurrence of mtDNA-encoded gene downregulation and nuclear OXPHOS gene upregulation, consistent with mitonuclear transcriptional imbalance.


A
GSEA Hallmark Pathways | GDM vs Control
GDMA1 + GDMA2 (n=14) vs Control (n=11)
OXIDATIVE PHOSPHORYLATION
DNA REPAIR
E2F TARGETS
FATTY ACID METABOLISM
MTORC1 SIGNALING
BILE ACID METABOLISM
ADIPOGENESIS
PROTEIN SECRETION
COMPLEMENT
APOPTOSIS
UV RESPONSE DN
TNFA SIGNALING VIA NFKB
TGF BETA SIGNALING
HYPOXIA
MYOGENESIS
MITOTIC SPINDLE
COAGULATION
APICAL JUNCTION
EPITHELIAL MESENCHYMAL TRANSITION
−2
−1
0
1
2
Normalized Enrichment Score (NES)
−log10(adj.P)
2
4
6
8
Down in GDM
Up in GDM

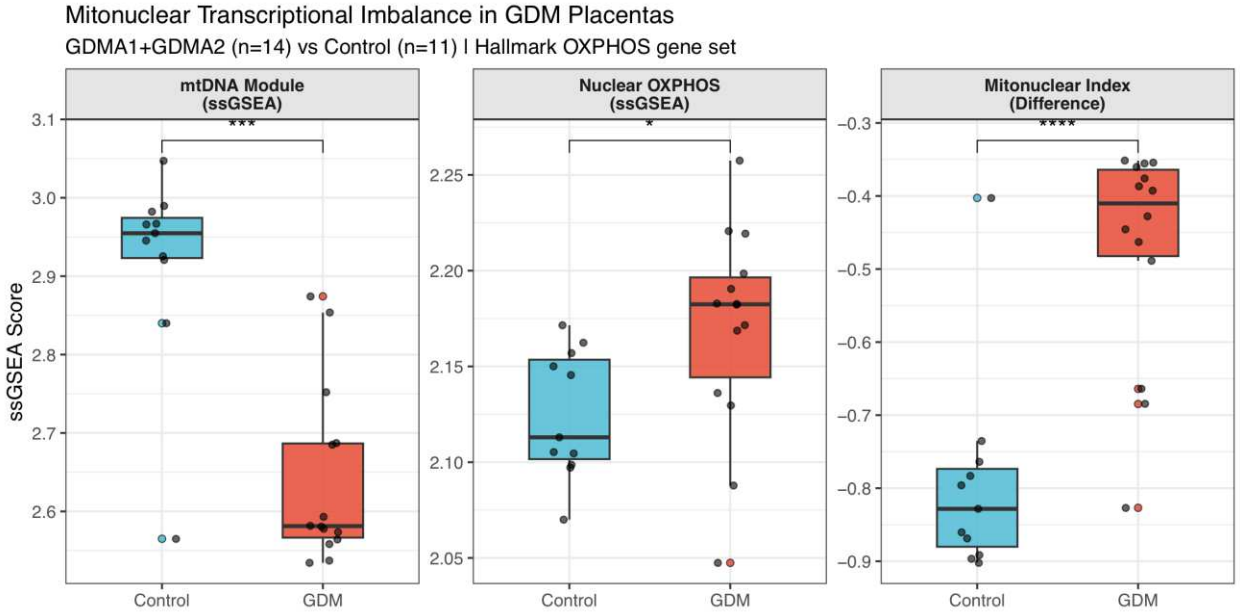

B
Key GSEA Pathways in GDM Placenta
pvalue
HALLMARK_EPITHELIAL_MESENCHYMAL_TRANSITION
1.000e−10
HALLMARK_OXIDATIVE_PHOSPHORYLATION
4.755e−10
Running Enrichment Score
0.25
0.00
−0.25
−0.50
Ranked List Metric
4
0
−4
−8
5000
10000
15000
Rank in Ordered Dataset

3.3 GDM Placentas Exhibit Pronounced Mitonuclear Transcriptional Imbalance

To visualize the divergent expression patterns of mtDNA-encoded and nuclear OXPHOS genes, we constructed a heatmap displaying the 13 mtDNA-encoded genes alongside representative nuclear genome-encoded OXPHOS genes (selected from the Hallmark OXPHOS gene set) across GDM and control samples (Figure 3). The two gene categories showed strikingly opposite expression patterns: mtDNA-encoded genes were consistently lower in GDM samples while nuclear OXPHOS genes were consistently higher, forming a clear and reproducible visual signature of mitonuclear imbalance.



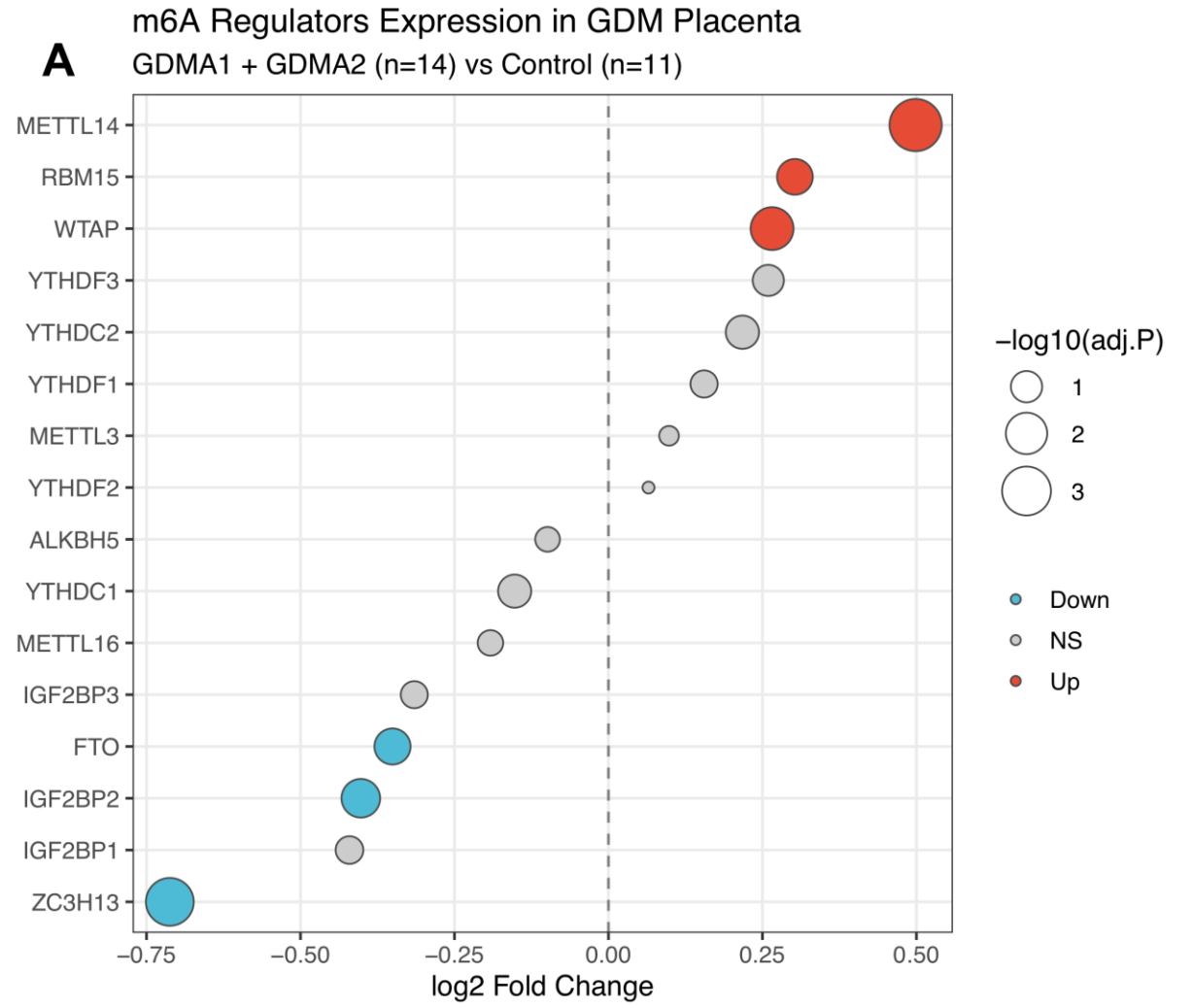
To quantify this phenomenon in a platform-agnostic manner, we computed a Mitonuclear Index for each sample using ssGSEA scores for both gene modules, defined as the difference between the Nuclear OXPHOS ssGSEA score and the mtDNA ssGSEA score. This rank-based approach was chosen to enable cross-platform comparisons (Figure 4). The Mitonuclear Index was significantly elevated in GDM placentas compared with controls (GDM mean = −0.470 vs. Control mean = −0.794; Wilcoxon $P = 8.75 \times 10^{-5}$, rank-biserial r = 0.72), driven by both a significantly higher Nuclear OXPHOS score ($P < 0.0001$) and a significantly lower mtDNA score ($P < 0.05$) in GDM. These results suggest that mitonuclear transcriptional imbalance represents a consistent transcriptional pattern in GDM placentas in this dataset, which warrants replication in independent cohorts.

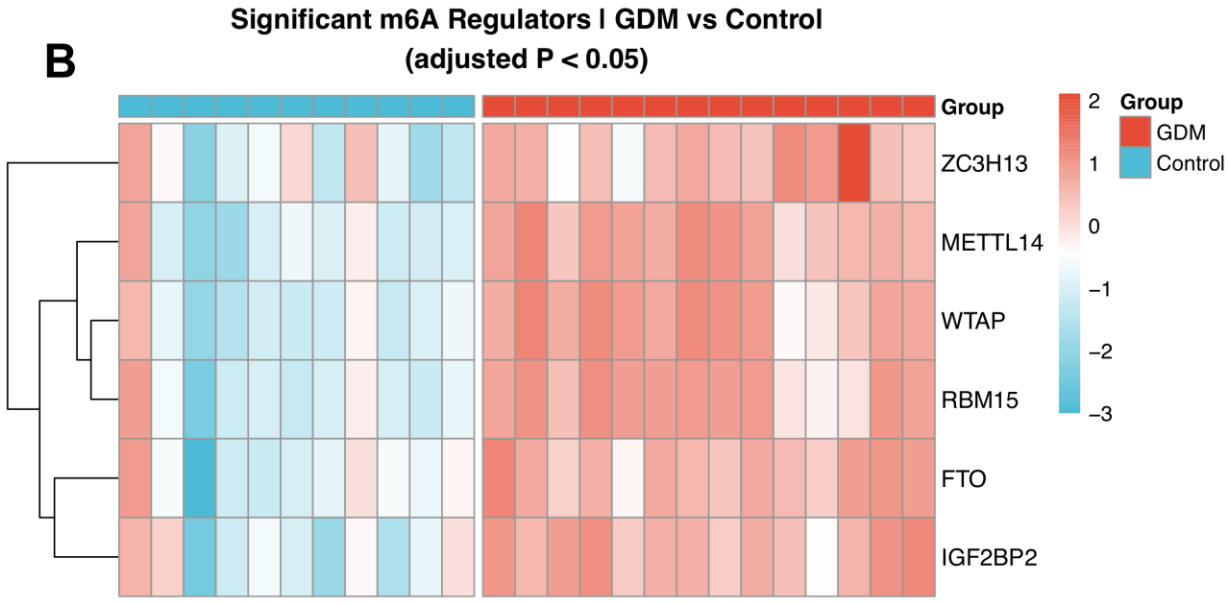


3.4 Widespread Dysregulation of m6A Regulatory Genes in GDM Placentas

Having observed a consistent pattern of mitonuclear transcriptional imbalance in GDM placentas, we investigated whether epitranscriptomic mechanisms might contribute to this metabolic reprogramming. Systematic evaluation of 16 m6A regulatory genes revealed significant differential expression of 6 genes (adjusted $P < 0.05$) (Figure 5A and 5B). Among writer complex components, *METTL14* showed the most significant upregulation ($\log^2FC = 0.499$, adjusted $P = 2.93 \times 10^{-4}$), followed by *WTAP* ($\log^2FC = 0.266$, adjusted $P = 6.66 \times 10^{-3}$) and *RBM15* ($\log^2FC = 0.303$, adjusted $P = 0.041$). In contrast, *ZC3H13* was significantly downregulated ($\log^2FC =$

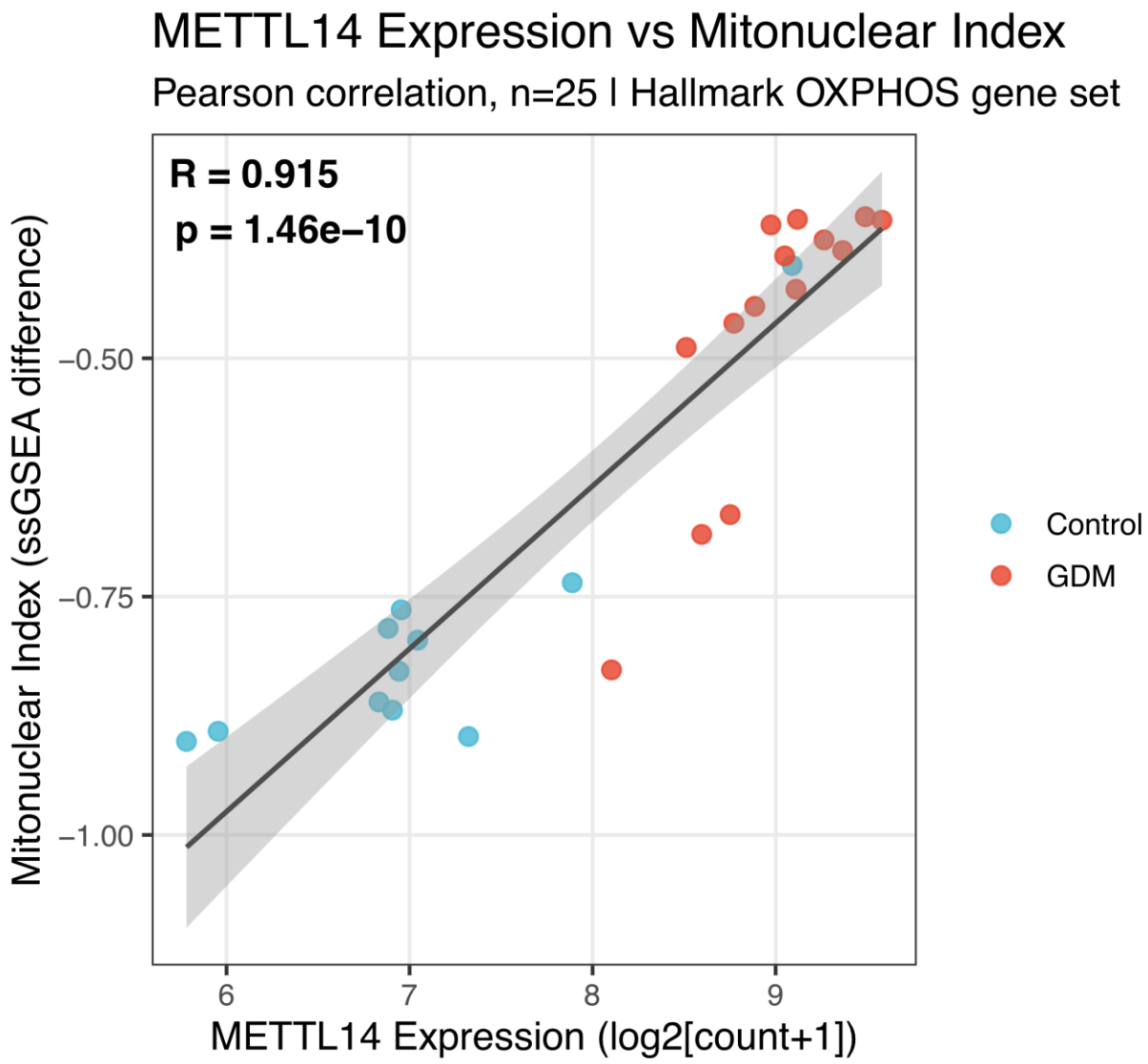
−0.712, adjusted P = 1.42×10^{-3}). Among erasers, *FTO* was downregulated ($\log^2$FC = −0.351, adjusted P = 0.038) and the reader *IGF2BP2* was downregulated ($\log^2$FC = −0.402, adjusted P = 0.021). These findings indicate broad perturbation of the m6A epitranscriptomic landscape in GDM placentas.


A
m6A Regulators Expression in GDM Placenta
GDMA1 + GDMA2 (n=14) vs Control (n=11)
METTL14
RBM15
WTAP
YTHDF3
YTHDC2
YTHDF1
METTL3
YTHDF2
ALKBH5
YTHDC1
METTL16
IGF2BP3
FTO
IGF2BP2
IGF2BP1
ZC3H13
−0.75
−0.50
−0.25
0.00
0.25
0.50
log2 Fold Change
−log10(adj.P)
1
2
3
Down
NS
Up


B
Significant m6A Regulators | GDM vs Control
(adjusted P < 0.05)
Group
ZC3H13
METTL14
WTAP
RBM15
FTO
IGF2BP2
2
1
0
−1
−2
−3
Group
GDM
Control

3.5 m6A Regulatory Gene Expression Co-occurs with the Mitonuclear Transcriptional State

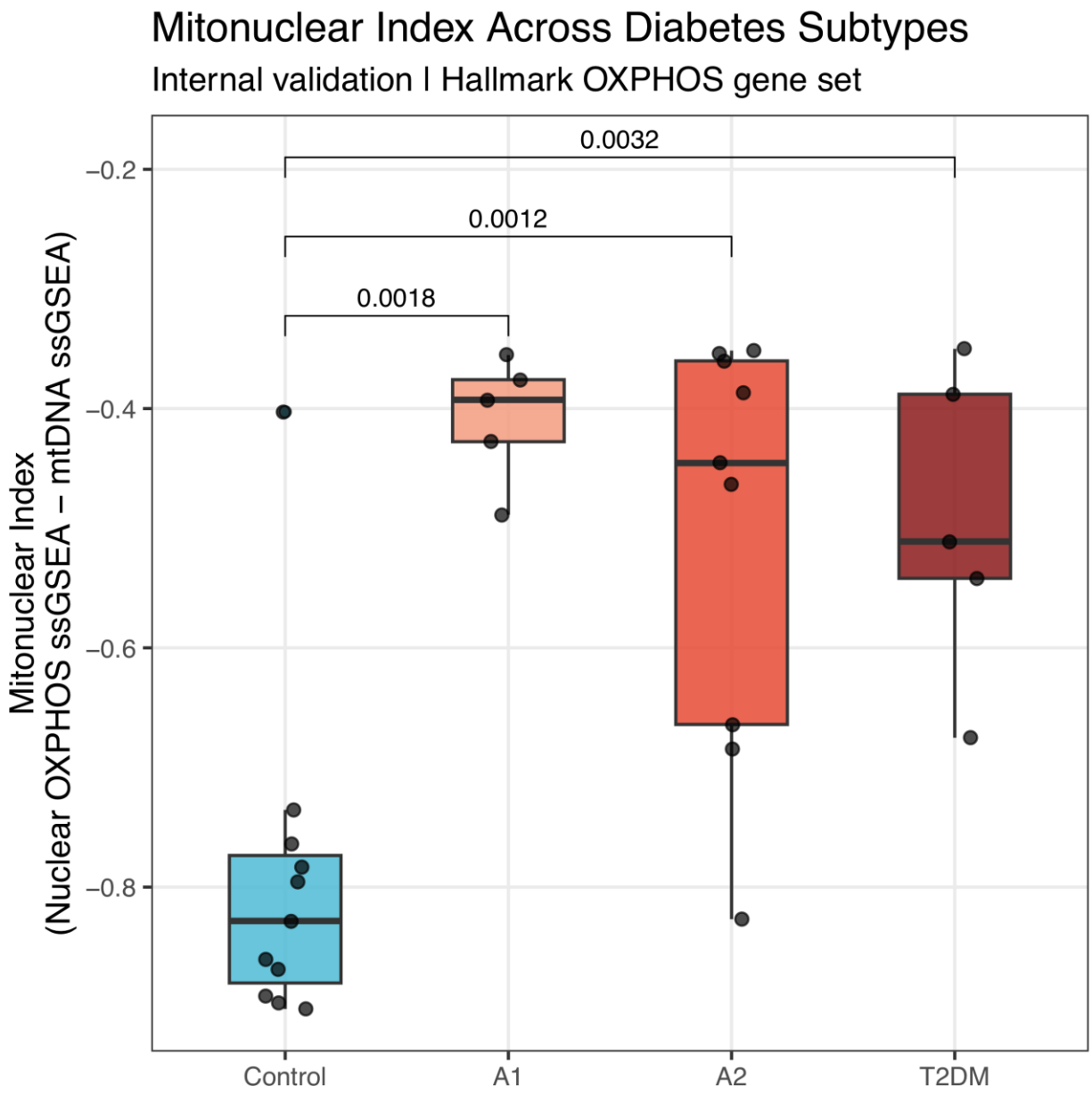
To explore whether m6A regulatory gene dysregulation was associated with the mitonuclear transcriptional phenotype, we examined the Pearson correlation between *METTL14* expression and the Mitonuclear Index across all 25 samples (Figure 6). A strong positive correlation was observed ($R = 0.915$, $P = 1.46 \times 10^{-10}$): samples with higher *METTL14* expression consistently showed higher Mitonuclear Index values, with GDM samples clustering at the high end of both axes.



To assess whether this correlation was specific to the Nuclear OXPHOS module or reflected a broader co-expression pattern, we performed a permutation test in which 1,000 random gene sets of size 200 were drawn from all expressed genes and their mean expression correlated with *METTL14*. The observed correlation fell within the distribution of random correlations (random mean R = 0.977 ± 0.002, empirical P = 1.0), indicating that the high correlation between *METTL14* and the Mitonuclear Index largely reflects the shared GDM transcriptional context rather than a specific association with the OXPHOS module. Consistently, *METTL14* expression was not significantly correlated with the mtDNA module score (R = 0.305, P = 0.14), indicating that *METTL14* upregulation does not directly predict the degree of mtDNA-encoded gene suppression. Together, these findings indicate that *METTL14* upregulation and mitonuclear transcriptional imbalance represent coordinately altered features of GDM placentas, consistent with a shared upstream regulatory context, rather than a direct regulatory relationship between *METTL14* and mitonuclear gene expression balance.

3.6 Mitonuclear Imbalance Is Observed Consistently across Hyperglycemia Subgroups within GSE249311

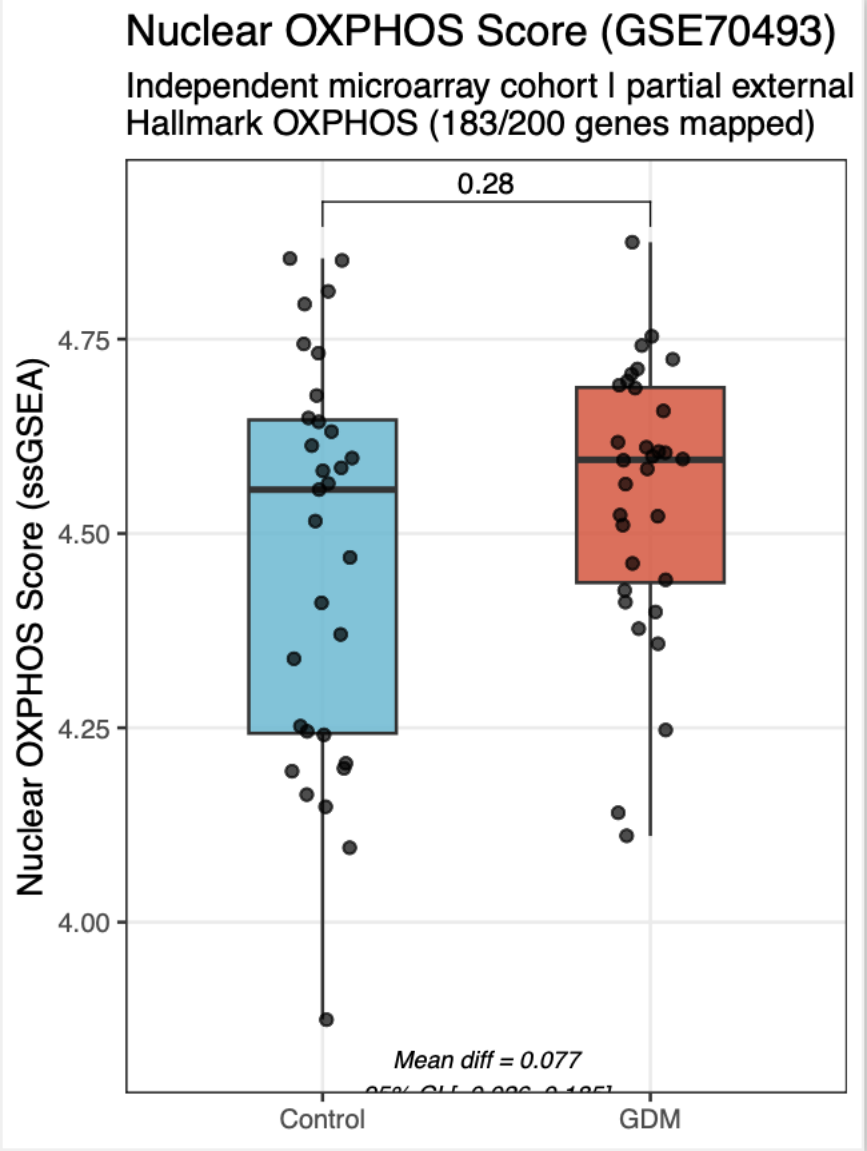
To assess robustness across different forms of pregnancy-associated hyperglycemia, we computed the Mitonuclear Index for all four subgroups within GSE249311: normoglycemic controls (n = 11), GDMA1 (n = 5), GDMA2 (n = 9), and T2DM in pregnancy (n = 5) (Figure 7). All three hyperglycemic subtypes showed significantly elevated Mitonuclear Index compared with controls: GDMA1 (Wilcoxon exact P = 0.0018, Bonferroni-corrected P = 0.0055), GDMA2 (Wilcoxon exact P = 0.0012, Bonferroni-corrected P = 0.0035), and T2DM (Wilcoxon exact P = 0.0032, Bonferroni-corrected P = 0.0096)). Notably, GDMA1 showed the most pronounced elevation despite being the milder, diet-controlled subtype. These findings demonstrate that mitonuclear transcriptional imbalance is a consistent transcriptional phenotype associated with maternal hyperglycemia during pregnancy, not restricted to a specific GDM subtype.



3.7 Nuclear OXPHOS Upregulation Shows Directional Consistency in an Independent Cohort Assessment

To assess the directional consistency of the nuclear OXPHOS component of mitonuclear imbalance in an independent cohort, we analyzed the placental microarray dataset GSE70493 (GDM n = 32, Control n = 31) (Supplementary Fig. S1). As the Affymetrix HTA 2.0 platform does not include probes for mtDNA-encoded genes, only the Nuclear OXPHOS ssGSEA score could be computed. The Nuclear OXPHOS score was directionally consistent with the primary analysis:

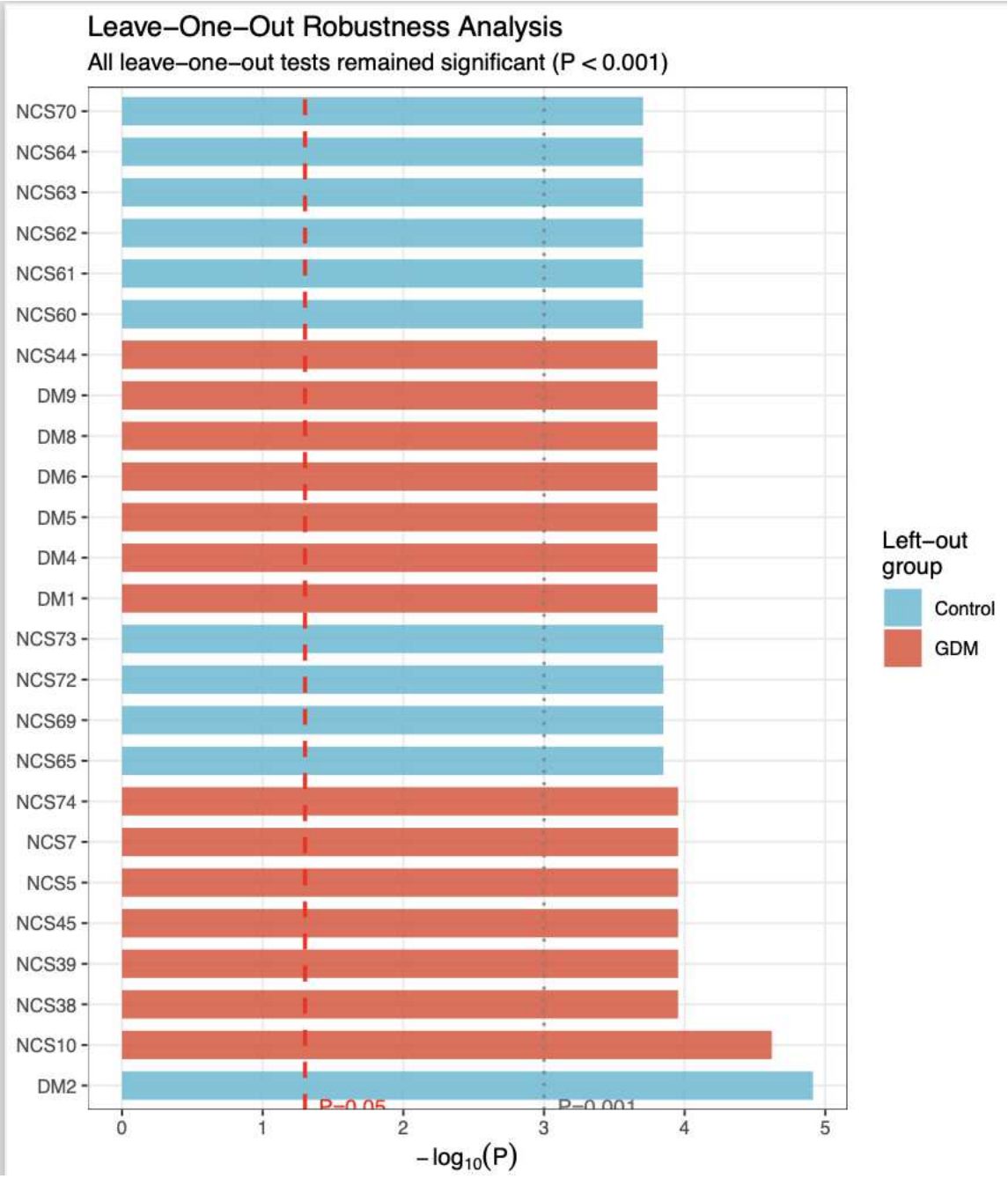
GDM placentas showed higher Nuclear OXPHOS scores than controls (GDM mean = 4.548 vs. Control mean = 4.471), although the difference did not reach statistical significance (Wilcoxon P = 0.28), consistent with the lower dynamic range of microarray platforms and the absence of the mtDNA component. Nevertheless, the directional consistency across two independent datasets and across three diabetes subtypes provides preliminary support for the internal consistency of nuclear OXPHOS upregulation as a transcriptional feature of GDM placentas within this dataset.



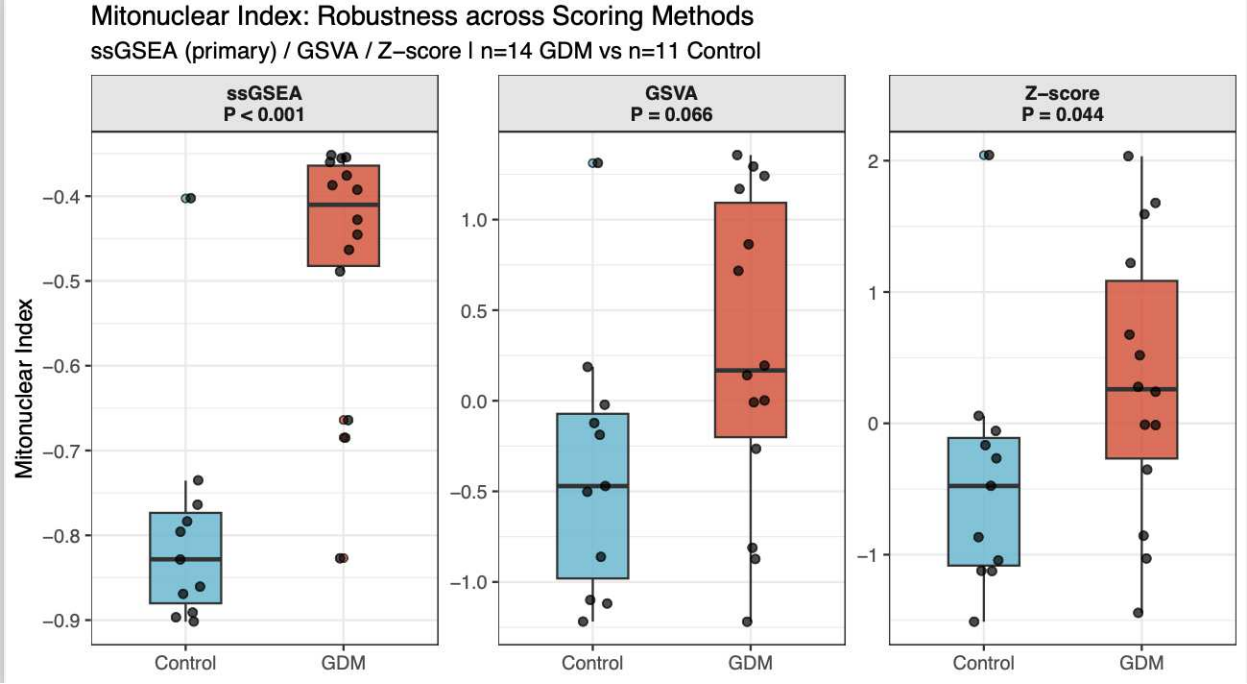
3.8 Robustness of the Mitonuclear Index across Analytical Approaches

To assess whether the observed mitonuclear transcriptional imbalance was robust to potential sample-level outliers and to the choice of scoring algorithm, three complementary robustness analyses were performed.

First, leave-one-out (LOO) analysis demonstrated that the significance of the GDM versus control Mitonuclear Index difference was preserved when any single sample was withheld: all 25 LOO iterations yielded Wilcoxon $P < 0.001$ (range: 1.22×10^{-5} to 1.98×10^{-4}), indicating that no individual sample exerted undue influence on the result (Supplementary Fig. S2).



Second, recomputing the Mitonuclear Index using two alternative scoring algorithms yielded concordant results across all three methods: ssGSEA ($P < 0.001$, rank-biserial $r = 0.723$), Z-score module score ($P = 0.044$, $r = 0.405$), and GSVA ($P = 0.066$, $r = 0.372$) (Supplementary Fig. S3). Although the GSVA result did not reach the conventional significance threshold, the direction and effect size were concordant with the primary analysis. The three scoring methods showed high pairwise correlations (ssGSEA–GSVA: $r = 0.812$; ssGSEA–Z-score: $r = 0.801$; GSVA–Z-score: $r = 0.978$), confirming that the mitonuclear imbalance signal is not an artifact of the ssGSEA algorithm.



Third, a more detailed assessment of the independent cohort GSE70493 revealed a mean difference in Nuclear OXPHOS scores of 0.077 (GDM = 4.548, Control = 4.471; 95% bootstrap CI: −0.026 to 0.185), with a small effect size (rank-biserial $r = 0.137$) and Wilcoxon $P = 0.28$ (Supplementary Fig. S1). The confidence interval, while including zero, is consistent with a small positive effect. The attenuated result in this dataset is expected given the lower dynamic range of microarray platforms and the absence of mtDNA probes precluding computation of the complete Mitonuclear Index.

4. Discussion

In this study, we performed a systematic transcriptomic analysis of placental tissue from women with gestational diabetes mellitus using the publicly available RNA-seq dataset GSE249311[10]. Our principal findings are as follows. First, all 13 mtDNA-encoded respiratory chain genes were significantly downregulated in GDM placentas, while nuclear genome-encoded OXPHOS genes were the most significantly upregulated pathway by GSEA. Second, quantifying this divergence

using a rank-based Mitonuclear Index revealed a highly significant elevation in GDM compared with controls (Wilcoxon P = 8.75 × 10−5). Third, this mitonuclear imbalance phenotype was consistently observed across all three hyperglycemic subgroups — GDMA1 (Wilcoxon exact P = 0.0018), GDMA2 (P = 0.0012), and T2DM in pregnancy (P = 0.0032) — suggesting it is a shared feature of maternal hyperglycemia rather than a subtype-specific phenomenon. Fourth, we identified widespread dysregulation of m6A regulatory genes in GDM placentas, with upregulation of writers METTL14, WTAP, and RBM15, and downregulation of ZC3H13, FTO, and IGF2BP2, indicating broad epitranscriptomic remodeling co-occurring with mitonuclear imbalance. To our knowledge, mitonuclear transcriptional imbalance has not previously been described as a placental transcriptional phenotype in the context of maternal hyperglycemia.

Mitochondrial dysfunction is a well-established feature of GDM placentas. Prior studies have demonstrated elevated reactive oxygen species (ROS) production, increased oxidative stress markers including 8-isoprostane and superoxide dismutase activity, and oxidative DNA damage in GDM placental tissue[16]. Placental trophoblasts from GDM and obese pregnancies exhibit altered mitochondrial respiration, reduced expression of mitochondrial complexes I–V, and impaired metabolic flexibility[4]. Placental mtDNA copy number has been associated with oxidative DNA damage in GDM placentas, suggesting a mechanistic link between oxidative stress and mitochondrial integrity[17]. Furthermore, oxidative stress-induced damage to mtDNA can activate the cGAS–STING innate immune pathway, amplifying inflammatory signaling and perpetuating a chronic inflammatory state in the placenta[18]. However, prior work has predominantly focused on mitochondrial respiratory capacity and ROS production in isolation, without systematically examining the coordinated relationship between mtDNA-encoded and nuclear genome-encoded gene expression. Our transcriptomic analysis addresses this gap.

The OXPHOS system is unique in that its constituent complexes are assembled from subunits encoded by two distinct genomes: the mitochondrial genome (encoding 13 core subunits) and the nuclear genome (encoding the remaining ∼70 structural subunits and hundreds of assembly factors)[19]. Proper OXPHOS function requires precise co-regulation of gene expression across these two compartments. Dysregulation of this balance termed mitonuclear imbalance has been documented in several pathological contexts. In aging, mitonuclear mismatch causes mitochondrial dysfunction and increased ROS production, effects that are exacerbated with

advancing age[5]. In obesity and type 2 diabetes, GSEA of skeletal muscle transcriptomes has identified the OXPHOS gene set as among the most significantly altered pathways, with complex patterns of differential regulation across the two genomic compartments[6]. In neurodegenerative diseases, mitonuclear incompatibilities arising from mutations in either genome can cause severe mitochondrial disease syndromes through disruption of OXPHOS complex assembly[20]. Our data reveal a specific and consistent pattern of mitonuclear transcriptional imbalance in GDM placentas: all 13 mtDNA-encoded respiratory chain genes were significantly downregulated (log2FC ≈ −1.4, adjusted $P < 10-9$), while nuclear genome-encoded OXPHOS genes were the most significantly upregulated pathway (NES = 2.15, adjusted $P = 1.19 \times 10-8$), driven by leading-edge genes including MRPL35, TIMM9, NDUFA5, and NDUFB5. These two gene categories are entirely non-overlapping, confirming that the divergence reflects genuine transcriptional uncoupling rather than an artifact of gene set composition. We propose that this pattern may reflect a compensatory nuclear response to impaired mtDNA transcription, analogous to retrograde mitochondria-to-nucleus signaling observed in other models of mitochondrial stress, although direct evidence for such compensatory signaling was not assessed in the present study[21].

Several non-mutually exclusive mechanisms may account for the observed reduction in mtDNA-encoded gene expression alongside concurrent nuclear OXPHOS upregulation. First, hyperglycemia-associated oxidative stress may contribute to reduced mtDNA-encoded gene expression, possibly through ROS-mediated mtDNA damage; oxidatively modified mtDNA has been associated with reduced transcriptional output in other contexts[18]. Superoxide anions induce 8-hydroxy-2′-deoxyguanosine formation, increasing mtDNA mutation rates and impairing transcription of ND1 and ND6[18]. Second, impaired mtDNA transcription may trigger retrograde mitochondria-to-nucleus signaling, a conserved stress response in which the nuclear genome upregulates mitochondrial biogenesis and OXPHOS assembly genes, mediated by factors including AMPK, mTORC1, and PGC-1α consistent with the HALLMARK_MTORC1_SIGNALING upregulation we observed (NES = 1.75). Third, GDM placentas may exhibit altered mitochondrial dynamics; a recent study reported dysregulation of mitochondrial structure dynamics, quality control, and clearance in GDM placentas, with a reduction in mitochondrial complex expression and failure of mitophagy pathways[4]. Fourth, the divergence may in part reflect differences in RNA kinetics: nuclear-encoded OXPHOS transcripts have much faster turnover and transcriptional responsiveness than polycistronic mtDNA

transcripts, which could amplify apparent differences in steady-state transcript levels[19]. Future studies directly measuring mtDNA copy number, mtDNA transcription rate, and OXPHOS protein assembly in GDM placentas will be important to distinguish these mechanisms.

m6A modification has emerged as an important regulator of mitochondrial homeostasis. A recent review established that m6A modification of transcripts encoding mitochondrial complex subunits regulates their translation efficiency through polysome association, with YTHDF family readers mediating this process[9]. Silencing METTL14 alleviates liver injury in non-alcoholic fatty liver disease by regulating mitochondrial homeostasis and dynamics[22], and METTL14 has been identified as a posttranscriptional regulator of hepatic glucose production through m6A-mediated regulation of G6pc in diet-induced obesity[23]. In our dataset, significant upregulation of METTL14, WTAP, and RBM15, alongside downregulation of FTO and IGF2BP2, indicates that m^{6}A epitranscriptomic remodeling co-occurs with mitonuclear transcriptional imbalance in GDM placentas, although permutation analysis established that this co-occurrence reflects the broader GDM transcriptional context rather than a specific regulatory link between the m^{6}A machinery and the mitonuclear state. Specifically, a permutation analysis demonstrated that the correlation between METTL14 expression and the Mitonuclear Index was not specific to the Nuclear OXPHOS module and largely reflected the broader GDM transcriptional context. Furthermore, METTL14 expression was not significantly correlated with the mtDNA module score ($R = 0.305$, $P = 0.14$). We therefore interpret m6A dysregulation and mitonuclear imbalance as coordinately altered features of GDM placentas, rather than evidence of a direct regulatory relationship.

The m6A regulatory landscape we identified is consistent with prior work on epitranscriptomic regulation in gestational complications. Upregulation of METTL14 has been reported to contribute to trophoblast dysfunction in preeclampsia by elevating FOXO3a expression in an m6A-dependent manner[7]. METTL3 is essential for trophoblast stem cell self-renewal and differentiation during human placentation[8]. In the specific context of GDM, METTL3 mediates m6A modification of hsa_circ_0072380 to regulate GDM progression[24], and RBM15 suppresses hepatic insulin sensitivity in offspring of GDM pregnancies through m6A-mediated regulation of CLDN4[25]. In hyperglycemic trophoblasts, METTL14 and ALKBH5 mRNA were significantly increased while WTAP decreased[26], partially consistent with our bulk RNA-seq findings. Together, the evidence suggests that m6A epitranscriptomic remodeling is a recurrent feature of the hyperglycemic

placenta, though the specific targets and consequences likely differ by cell type and gestational context.

The original study from which GSE249311 was derived aimed to determine whether GDMA1 and GDMA2 represent biologically distinct entities or a continuous spectrum[10]. Our analysis complements this question: the mitonuclear transcriptional imbalance phenotype was consistently elevated across all three hyperglycemic subgroups, with GDMA1 (diet-controlled) showing the most pronounced elevation despite being the clinically milder subtype. This suggests that mitonuclear transcriptional imbalance may represent a placental adaptation to maternal hyperglycemia per se, independent of pharmacological management or disease severity, and may help explain why prior studies using mixed or unclassified GDM cohorts have yielded inconsistent transcriptomic findings.

Several limitations warrant consideration. First, the primary analysis is based on a single dataset (GSE249311, n = 25), and while internal subtype analysis and an independent cohort assessment in GSE70493 provided directional, non-significant consistency, formal replication in a larger independent RNA-seq cohort remains important. Second, bulk RNA-seq captures the aggregate signal of all placental cell types; whether mitonuclear imbalance is driven by a specific cell population requires single-cell or spatial transcriptomic resolution. Additionally, changes in mtDNA-encoded transcript levels in bulk RNA-seq may be influenced by technical factors including mitochondrial RNA degradation, tissue ischemia time, and variation in placental cell composition, which cannot be distinguished from true transcriptional changes without complementary assays such as mtDNA copy number quantification or mitochondrial transcription rate measurement. Third, this study is observational: we did not perform functional experiments to establish causal relationships between mitonuclear imbalance, m6A dysregulation, and placental outcomes. Fourth, clinical metadata including maternal BMI, gestational age, fetal sex, delivery mode, and pharmacological treatment were not available in the GEO deposit of GSE249311, precluding covariate-adjusted sensitivity analyses. Future studies should prospectively collect and deposit these variables to enable more rigorous confounding control. Future studies incorporating mtDNA copy number quantification, mitochondrial respiration assays, and MeRIP-seq in GDM placental samples or trophoblast cell models will be necessary to establish functional significance.

Conclusion

Our findings suggest mitonuclear transcriptional imbalance, characterized by concurrent downregulation of mtDNA-encoded respiratory chain genes and upregulation of nuclear genome-encoded OXPHOS components, as a candidate placental transcriptional phenotype observed consistently across subgroups within GSE249311, including GDM subtypes and T2DM in pregnancy. This phenotype co-occurs with widespread m6A epitranscriptomic remodeling, including upregulation of the m6A writer METTL14 and dysregulation of multiple reader and eraser components. Future mechanistic studies are warranted to determine whether impaired mtDNA transcription, retrograde mitochondrial signaling, and epitranscriptomic remodeling jointly contribute to placental adaptation and dysfunction in gestational diabetes mellitus.

Figure Legends

Figure 1. Transcriptomic landscape of GDM placentas revealed by differential expression analysis. Volcano plot showing differentially expressed genes (DEGs) in GDM placentas (GDMA1 + GDMA2, n = 14) compared with normoglycemic controls (n = 11) from GSE249311. Red dots indicate significantly upregulated genes ($\log^2$FC > 1, adjusted P < 0.05, n = 151); blue dots indicate significantly downregulated genes ($\log^2$FC < −1, adjusted P < 0.05, n = 760); grey dots indicate non-significant genes. Selected genes of interest are labeled, including mtDNA-encoded respiratory chain genes (*MT-ND1, MT-CO1, MT-CYB, MT-ATP6*), nuclear OXPHOS genes (*MRPL35, NDUFA5, TIMM9*), m6A regulatory genes (*METTL14, WTAP, ZC3H13, FTO, IGF2BP2, RBM15*), and other notable DEGs (*FN1, NEAT1*). Dashed vertical lines indicate $|\log^2\text{FC}| = 1$; dashed horizontal line indicates adjusted P = 0.05. DEG, differentially expressed gene; GDM, gestational diabetes mellitus.

Figure 2. Pathway-level transcriptional alterations in GDM placentas identified by GSEA. (A) Dot plot showing all 19 significantly enriched Hallmark gene sets (adjusted P < 0.05) in GDM versus control placentas. The x-axis shows the normalized enrichment score (NES); dot size represents $-\log^{10}$(adjusted P); red dots indicate pathways upregulated in GDM; blue dots indicate pathways downregulated in GDM. (B) Enrichment score curves for the four most significantly enriched pathways: HALLMARK_OXIDATIVE_PHOSPHORYLATION (NES = 2.15), HALLMARK_EPITHELIAL_MESENCHYMAL_TRANSITION (NES = −2.55),

HALLMARK_FATTY_ACID_METABOLISM (NES = 1.76), and HALLMARK_MTORC1_SIGNALING (NES = 1.75). The x-axis shows rank in the ordered gene list (ranked by DESeq2 Wald test statistic); the lower panel shows the ranked list metric. GSEA, gene set enrichment analysis; NES, normalized enrichment score.

Figure 3. Mitonuclear transcriptional imbalance in GDM placentas. Heatmap displaying Z-score-scaled expression of 13 mtDNA-encoded respiratory chain genes (upper panel, orange annotation bar) and representative nuclear genome-encoded OXPHOS genes from the predefined Hallmark OXPHOS gene set (lower panel, blue annotation bar) across GDM (n = 14, red) and control (n = 11, blue) placental samples. Samples are ordered by group (Control, left; GDM, right) without hierarchical clustering; genes are ordered by category. Color scale represents Z-score of $\log^2$-normalized counts (blue, low expression; red, high expression). The two gene categories exhibit strikingly opposite expression patterns across groups. A gap line separates the two gene categories. mtDNA, mitochondrial DNA; OXPHOS, oxidative phosphorylation.

Figure 4. Quantification of mitonuclear transcriptional imbalance using the Mitonuclear Index. Boxplots showing the mtDNA module score (left), Nuclear OXPHOS score (middle), and Mitonuclear Index (right) in GDM (n = 14, red) and control (n = 11, blue) placentas. Both the mtDNA module score and Nuclear OXPHOS score were computed using single-sample gene set enrichment analysis (ssGSEA). The Mitonuclear Index is defined as the difference between the Nuclear OXPHOS ssGSEA score and the mtDNA ssGSEA score (Nuclear OXPHOS module: Hallmark OXIDATIVE_PHOSPHORYLATION gene set, MSigDB, n = 200). Individual data points are overlaid on boxplots. Statistical significance was assessed by two-tailed Wilcoxon rank-sum test; * $P < 0.05$, *** $P < 0.001$, **** $P < 0.0001$. Effect size is reported as rank-biserial correlation (r = 0.72 for GDM vs. Control). ssGSEA, single-sample gene set enrichment analysis.

Figure 5. Widespread dysregulation of m6A regulatory genes in GDM placentas. (A) Bubble plot showing differential expression of 16 m6A regulatory genes in GDM versus control placentas. The x-axis shows $\log^2$ fold change; the y-axis shows gene identity ordered by $\log^2$FC. Dot size represents $-\log^{10}$(adjusted P); red dots indicate significantly upregulated genes (adjusted $P < 0.05$); blue dots indicate significantly downregulated genes; grey dots indicate non-significant genes. (B) Heatmap showing Z-score-scaled expression of six significantly dysregulated m6A regulatory

genes (adjusted $P < 0.05$) across GDM (n = 14, red) and control (n = 11, blue) samples. Samples are ordered by group; genes are clustered by hierarchical clustering. Color scale represents Z-score (blue, low; red, high). m6A, N6-methyladenosine; GDM, gestational diabetes mellitus.

Figure 6. Correlation between *METTL14* expression and the Mitonuclear Index. Scatter plot showing the Pearson correlation between *METTL14* $\log^2$-normalized expression (x-axis) and the Mitonuclear Index (y-axis) across all 25 samples (GDM, n = 14, red; Control, n = 11, blue). The solid line represents the linear regression fit; the shaded area represents the 95% confidence interval. Pearson correlation coefficient (R) and P value are shown. The Mitonuclear Index is defined as the ssGSEA difference score (Nuclear OXPHOS score − mtDNA score). ssGSEA, single-sample gene set enrichment analysis.

Figure 7. Internal subgroup assessment of mitonuclear transcriptional imbalance across diabetes subtypes. Boxplot showing the Mitonuclear Index in normoglycemic controls (Control, n = 11, blue), GDMA1 (n = 5, light orange), GDMA2 (n = 9, red), and type 2 diabetes mellitus in pregnancy (T2DM, n = 5, dark red) from GSE249311. Individual data points are overlaid on boxplots. Statistical significance was assessed by two-tailed Wilcoxon rank-sum test (exact) for each subtype versus Control; P values are shown above comparison brackets. The Mitonuclear Index is defined as the ssGSEA difference score (Nuclear OXPHOS score − mtDNA score). GDMA1, gestational diabetes subtype A1 (diet-controlled); GDMA2, gestational diabetes subtype A2 (medication-requiring); T2DM, type 2 diabetes mellitus; ssGSEA, single-sample gene set enrichment analysis.

Supplementary Figure 1. Nuclear OXPHOS score in an independent placental cohort (GSE70493). Boxplot showing the Nuclear OXPHOS ssGSEA score in GDM (n = 32, red) and normoglycemic control (n = 31, blue) placental samples from the independent microarray dataset GSE70493 (Affymetrix Human Transcriptome Array 2.0). Individual data points are overlaid on boxplots. The Nuclear OXPHOS score was computed using ssGSEA with the Hallmark OXIDATIVE_PHOSPHORYLATION gene set (MSigDB), of which 183 out of 200 genes were present on the Affymetrix HTA 2.0 platform. The complete Mitonuclear Index could not be computed in this dataset as mtDNA-encoded genes are not represented on the Affymetrix HTA 2.0 platform. Statistical comparison was performed using a two-tailed Wilcoxon rank-sum test

(P = 0.28). The mean difference was 0.077 (95% bootstrap CI: −0.026 to 0.185; rank-biserial r = 0.137, small effect). The title reflects the partial nature of this assessment: only the nuclear OXPHOS component could be evaluated as mtDNA-encoded genes are absent from the Affymetrix HTA 2.0 platform. GDM, gestational diabetes mellitus; ssGSEA, single-sample gene set enrichment analysis; OXPHOS, oxidative phosphorylation.

Supplementary Figure 2. Leave-one-out robustness analysis of the Mitonuclear Index. Horizontal bar plot showing −log10(P) values from Wilcoxon rank-sum tests comparing GDM versus control Mitonuclear Index in each of 25 leave-one-out iterations, where one sample was withheld at a time. Bar color indicates the group of the withheld sample (GDM, red; Control, blue). The red dashed vertical line indicates P = 0.05; the grey dotted line indicates P = 0.001. All 25 leave-one-out tests remained significant (P < 0.001).

Supplementary Figure 3. Mitonuclear Index shows concordant directionality across three scoring methods. Boxplots showing the Mitonuclear Index in GDM (n = 14, red) and control (n = 11, blue) placentas computed using ssGSEA (primary method), GSVA, and Z-score module score. All three methods use the predefined Hallmark OXIDATIVE_PHOSPHORYLATION gene set (MSigDB, n = 200). P values are shown in panel headers. Pairwise correlations between methods: ssGSEA–GSVA r = 0.812; ssGSEA–Z-score r = 0.801; GSVA–Z-score r = 0.978.

Data Availability

All datasets analysed in this study are publicly available. The primary dataset GSE249311 is accessible via the NCBI GEO database at https://www.ncbi.nlm.nih.gov/geo/query/acc.cgi?acc=GSE249311. The secondary microarray dataset GSE70493 is accessible at https://www.ncbi.nlm.nih.gov/geo/query/acc.cgi?acc=GSE70493. R scripts used for all analyses are available from the corresponding author upon reasonable request.

Code Availability

R scripts used for the analyses described in this manuscript are available from the corresponding author upon reasonable request.

Ethics declarations

This study used only publicly available, de-identified transcriptomic data deposited in the NCBI Gene Expression Omnibus (GEO) database. No new human subjects were enrolled and no biological samples were collected. Ethics approval and informed consent were not required for this secondary analysis of publicly available data.

Author contributions

X.Z. conceived the study, performed all bioinformatics analyses, and drafted the manuscript. L.G. contributed to data interpretation and critically revised the manuscript. H.B. assisted with data collection and literature review. W.T. replicated the data analysis and contributed to result verification. X.C. supervised the study, provided critical intellectual input, and revised the manuscript. All authors reviewed the final manuscript.

Competing interests

The authors declare no competing interests.

Funding

This research received no external funding.

Acknowledgements

The authors thank the investigators who deposited the transcriptomic datasets GSE249311 and GSE70493 into the NCBI Gene Expression Omnibus database, making this secondary analysis possible. The authors used Claude (Anthropic, claude.ai) to assist with manuscript drafting and language editing. All content was verified and approved by the authors.

Additional information

Correspondence and requests for materials should be addressed to X.C. (chxf_1984@hotmail.com).

References

1. Sweeting, A. *et al.* Epidemiology and management of gestational diabetes. *Lancet* **404**, 175–192 (2024).
2. McIntyre, H. D. *et al.* Gestational diabetes mellitus. *Nat. Rev. Dis. Primer* **5**, 47 (2019).
3. Ni, D. & Nanan, R. Elucidating the maternal and fetal metabolic and immune landscapes of gestational diabetes mellitus with a pan-organ transcriptomic atlas. *Genes Dis.* **13**, 101551 (2026).

4. Kadam, L., Chan, K., Tawater, E. & Myatt, L. Dysregulation of placental mitochondrial structure dynamics and clearance in maternal obesity and gestational diabetes. *Placenta* **171**, 140–149 (2025).
5. Pichaud, N. *et al.* Age Dependent Dysfunction of Mitochondrial and ROS Metabolism Induced by Mitonuclear Mismatch. *Front. Genet.* **10**, 130 (2019).
6. Pinti, M. V. *et al.* Mitochondrial dysfunction in type 2 diabetes mellitus: an organ-based analysis. *Am. J. Physiol. Endocrinol. Metab.* **316**, E268–E285 (2019).
7. Fan, W. *et al.* Upregulation of METTL14 contributes to trophoblast dysfunction by elevating FOXO3a expression in an m6A-dependent manner. *Placenta* **124**, 18–27 (2022).
8. Kumar, R. P. *et al.* METTL3 shapes m6A epitranscriptomic landscape for successful human placentation. Preprint at https://doi.org/10.1101/2024.07.12.603294 (2024).
9. Yan, W., Saqirile, null, Li, K., Li, K. & Wang, C. The Role of N6-Methyladenosine in Mitochondrial Dysfunction and Pathology. *Int. J. Mol. Sci.* **26**, 3624 (2025).
10. Barrozo, E. R. *et al.* Discrete placental gene expression signatures accompany diabetic disease classifications during pregnancy. *Am. J. Obstet. Gynecol.* **232**, 326.e1-326.e15 (2025).
11. Love, M. I., Huber, W. & Anders, S. Moderated estimation of fold change and dispersion for RNA-seq data with DESeq2. *Genome Biol.* **15**, 550 (2014).
12. Wu, T. *et al.* clusterProfiler 4.0: A universal enrichment tool for interpreting omics data. *Innov. Camb. Mass* **2**, 100141 (2021).
13. Liberzon, A. *et al.* The Molecular Signatures Database (MSigDB) hallmark gene set collection. *Cell Syst.* **1**, 417–425 (2015).
14. Hänzelmann, S., Castelo, R. & Guinney, J. GSVA: gene set variation analysis for microarray and RNA-seq data. *BMC Bioinformatics* **14**, 7 (2013).

15. Binder, A. M., LaRocca, J., Lesseur, C., Marsit, C. J. & Michels, K. B. Epigenome-wide and transcriptome-wide analyses reveal gestational diabetes is associated with alterations in the human leukocyte antigen complex. *Clin. Epigenetics* **7**, 79 (2015).

16. Coughlan, M. T., Vervaart, P. P., Permezel, M., Georgiou, H. M. & Rice, G. E. Altered placental oxidative stress status in gestational diabetes mellitus. *Placenta* **25**, 78–84 (2004).

17. Qiu, C. *et al.* Mitochondrial DNA copy number and oxidative DNA damage in placental tissues from gestational diabetes and control pregnancies: a pilot study. *Clin. Lab.* **59**, 655–660 (2013).

18. Feng, Z., Tan, Z. & Lu, D. Mitochondrial bioenergetics dysfunction in T2DM: linking oxidative stress to insulin resistance. *Front. Endocrinol.* **16**, 1674477 (2025).

19. McShane, E. *et al.* A kinetic dichotomy between mitochondrial and nuclear gene expression processes. *Mol. Cell* **84**, 1541-1555.e11 (2024).

20. Gershoni, M. *et al.* Disrupting mitochondrial-nuclear coevolution affects OXPHOS complex I integrity and impacts human health. *Genome Biol. Evol.* **6**, 2665–2680 (2014).

21. Quirós, P. M., Mottis, A. & Auwerx, J. Mitonuclear communication in homeostasis and stress. *Nat. Rev. Mol. Cell Biol.* **17**, 213–226 (2016).

22. Wang, W., Yan, J., Han, L., Zou, Z.-L. & Xu, A.-L. Silencing METTL14 alleviates liver injury in non-alcoholic fatty liver disease by regulating mitochondrial homeostasis. *Biomol. Biomed.* **24**, 505–519 (2024).

23. Zheng, Q. *et al.* METTL14-Induced M6A Methylation Increases G6pc Biosynthesis, Hepatic Glucose Production and Metabolic Disorders in Obesity. *Adv. Sci.* **12**, e2417355 (2025).

24. Zhang, S. *et al.* METTL3 mediates m6A modification of hsa_circ_0072380 to regulate the progression of gestational diabetes mellitus. *Gene* **931**, 148894 (2024).

25. Fang, J. *et al.* RBM15 suppresses hepatic insulin sensitivity of offspring of gestational diabetes mellitus mice via m6A-mediated regulation of CLDN4. *Mol. Med.* **29**, 23 (2023).

26. Ning, J. *et al.* Demethylase FTO-mediated m6A modification of SIK1 modulates placental cytotrophoblast syncytialization in type 2 diabetes mellitus. *iScience* **27**, 109900 (2024).